Electrochemical and Solid-State Letters, **11** (10) H276-H279 (2008)
1099-0062/2008/11(10)/H276/4/$23.00 © The Electrochemical Society

Laser Annealing on Ti Electrode: Impact on $Ti/HfO_2/SiO_2$ n-Type MOSFET

Sungho Heo,[a,z] R. Dong,[a] Musarrat Hasan,[a] Hyunsang Hwang,[a,*] S. D. Park,[b] and G. Y. Yeom[b]

[a]*Department of Materials Science and Engineering, Gwangju Institute of Science and Technology, Buk-gu, Gwangju 500-712, Korea*
[b]*Department of Materials Science and Engineering, Sungkyunkwan University, Suwon, Kyunggi-do 440-746, Korea*

Low-thermal-budget processes are required for Ti electrode in the present gate-first n-channel metal-oxide-semiconductor field effect transistor (nMOSFET) applications because of its thermal stability problem. In this article, the effects of laser annealing on Ti electrodes (in HfO_2/SiO_2 nMOSFET) are discussed. The processes of Ti electrode degradation and HfO_2 crystallization are optimized effectively. HfO_2/SiO_2 nMOSFET with Ti electrode displayed an effective work function (~4.26 eV), corresponding to the conduction bandedge and an equivalent oxide thickness of 11.7 Å by controlling the laser annealing.
© 2008 The Electrochemical Society. [DOI: 10.1149/1.2960370] All rights reserved.

Manuscript submitted January 31, 2008; revised manuscript received June 27, 2008. Published July 25, 2008.

Metal gate electrodes with Hf-based high-*k* dielectrics have been intensively researched for metal-oxide-semiconductor field effect transistors (MOSFETs).[1] However, a remaining open issue, the thermal stability of the metal gate electrode after conventional high-temperature annealing (>1000°C), must be resolved before potential device applications can be considered. Therefore, nitride-based metal gate electrodes have been suggested for n-type MOSFETs (nMOSFETs). Nitride-based metal gate electrodes show the midgap work function after high-temperature annealing.[2] Pure Ti electrode, in contrast to nitride-based metal gate electrode, has a low vacuum work function (4.33 eV) and low resistivity.[3] Moreover, the equivalent oxide thickness (EOT) can be reduced even in low-temperature (>300°C) forming gas annealing (FGA) due to the effect of oxygen gettering.[4] In addition, Seo et al.[5] have demonstrated that the interfacial layer thickness, e.g., ~6 Å, can be reduced by using Ti electrode, and no significant increase is observed for the interface trap density (D_{it}). Although numerous potential advantages have been proposed, few studies have been performed for nMOSFETs because of the above-mentioned thermal stability problem.[2]

In this study, very short time laser annealings (LAs), e.g., approximately nanoseconds, were performed on HfO_2/SiO_2 nMOSFETs with Ti electrode to resolve the thermal stability problem. An Al capping layer was also employed on the Ti electrode to reduce the effective thermal budget. The Al capping layer is expected to reduce the laser absorption rate due to its high reflectivity (~92%) of Al.[6,7]

Experimental

A p-type Si wafer with a resistivity of 0.5–0.6 Ω cm ($\sim 3 \times 10^{16}/cm^3$) was used as a substrate and channel doping was not performed for Ti nMOSFET. A HfO_2 (3.1 nm) layer was deposited on chemical silicon dioxide (~6 Å) by atomic layer deposition (ALD) where tetrakis hafnium and O_3 gas act as the Hf precursor and oxidizing agent, respectively. Al (200 nm)/Ti (50 nm) stack electrode was deposited on HfO_2 via a cosputtering system. After HfO_2 etching in the source/drain area, phosphorus ion implantation was performed at an energy of 12 keV with a dose of $3 \times 10^{15}/cm^2$. Laser annealing was conducted via a KrF excimer laser with energy of 400–700 mJ/cm^2 at 1 pulse. The sheet resistance (R_s) and active carrier concentration were measured by Hall measurement. The Al/Ti stack structure was deposited as a source/drain electrode. FGA was performed at 400°C for 30 min. The electrical characteristics of capacitance–voltage (*C-V*) and current–voltage were evaluated using an HP 4284A and HP 4155C semiconductor parameter analyzer, respectively. High-resolution cross-sectional transmission electron microscopy (HR-XTEM) and glancing-incidence X-ray diffraction (GIXRD) analyses were conducted in order to confirm the structural properties of the HfO_2/SiO_2 n-type metal-oxide-semiconductor (nMOS) capacitor with Ti electrode after LA and FGA.

Results and Discussion

Figure 1a shows the R_s and dopant activation rate (%) after the LA process. A low R_s (~280Ω/□) value and a high activation rate (68%) were observed by applying LA at 500 mJ/cm^2. The authors have demonstrated that the laser energy of 500 mJ/cm^2 is equivalent to that of a temperature of ~1114°C.[8] Hence, laser energy, up to 500 mJ/cm^2, is suggested to be sufficient for dopant activation in the source/drain because of the recrystallization of the amorphous-Si (α-Si) layer. Figure 1b shows the *C-V* characteristics of a HfO_2/SiO_2 nMOS capacitor with Ti electrode after LA. From the *C-V* data, the flatband voltage (V_{fb}) and the EOT value can be extracted by the NCSU program,[9] as shown in Fig. 1c. In order to confirm the effect of the Ti electrode on a HfO_2/SiO_2 nMOS capacitor, a Pt nMOS capacitor was fabricated. A Pt electrode is known to experience only a negligible reaction with HfO_2 layers. Thus, an accurate EOT value can be extracted without a Ti electrode effect. Compared with a Pt nMOS capacitor, a Ti nMOS capacitor shows an EOT decrease (~4 Å). This decrease in the EOT may be caused by the Ti electrode effect.[4] The samples with LA show almost the same V_{fb} voltage (~0.72 V) as that of the samples without LA. This means that the oxide charge and interface quality are not significantly changed by LA. The V_{fb} voltage revealed that the laser-annealed Ti electrode could easily achieve an effective work function (~4.26 eV) corresponding with the conduction bandedge. Furthermore, a slight EOT increase (~1.5 Å) was demonstrated in the case of the samples with a LA at 600 mJ/cm^2 (equivalent temperature of ~1200°C). As the LA energy increases beyond 700 mJ/cm^2, the gate deformation becomes severe due to the intermixing between the metal electrode and the gate dielectric. Thus, an optimized LA is crucial for the gate-first MOSFET process.

HR-XTEM and GIXRD analyses were conducted to investigate the possible EOT changes and crystalline structures of HfO_2 for samples with and without LA, as shown in Fig. 2. In the HR-XTEM result, the sample without LA in Fig. 2b shows an interfacial layer (IL) with a thickness of 1.5 nm. During the ALD process, the growth of the SiO_x layer and the intermixing of the two layers between the chemical oxide and the HfO_2 occur. However, a TEM analysis cannot identify these layers. Bersuker et al.[10] demonstrated

* Electrochemical Society Active Member.
[z] E-mail: kojiro@gist.ac.kr

Downloaded 11 Aug 2008 to 61.72.111.1. Redistribution subject to ECS license or copyright; see http://www.ecsdl.org/terms_use.jsp

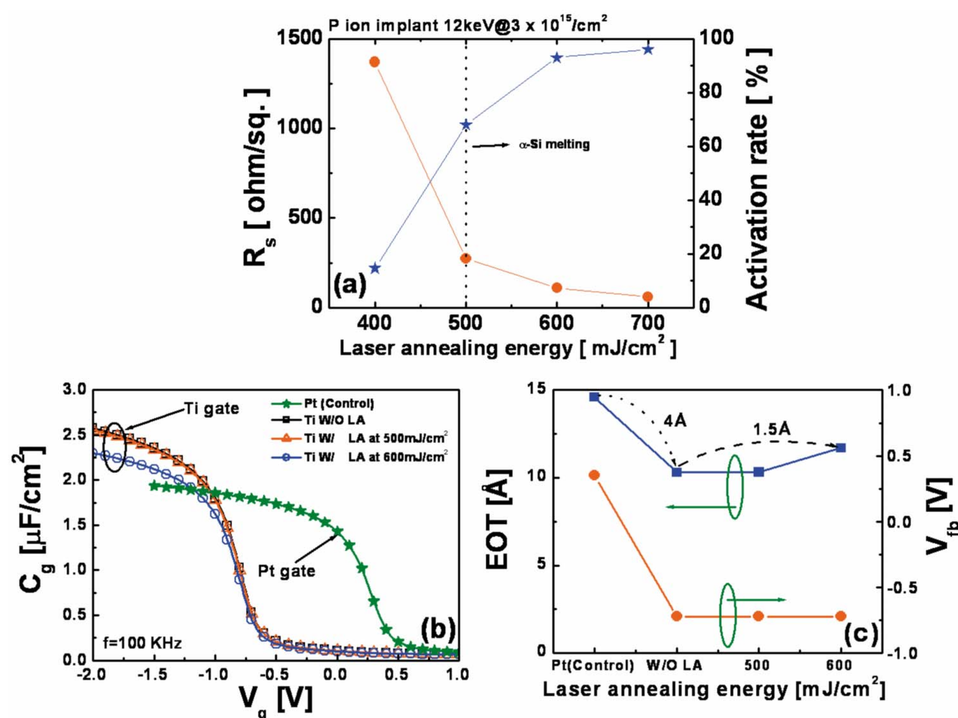

Figure 1. (Color online) (a) Variation of sheet resistance (R_s) and activation rate (%) as a function of LA energy of 400–700 mJ/cm^2 with one pulse. (b) *C-V* characteristics of the nMOS capacitor samples with (W/) or without (W/O) LA. (c) EOT and V_{fb} vs LA energy.

that process-grown layers of a Hf-silicate or SiO_x layer have a dielectric constant that is 3–4 times higher compared to bulk SiO_2 ($k = 3.9$). Additionally, the EOT value is similar to the IL thickness. Our Pt nMOS capacitor sample also shows a similar EOT value ($\sim$1.46 nm) to IL thickness ($\sim$1.5 nm), as shown in Fig. 2d. LAs can effectively reduce the growth of ILs, because LAs have relatively short annealing time compared with those of conventional activation annealing.[11] Moreover, it is well known that the thickness ($\sim$2 Å) of the SiO_2 IL will be increased if the applied laser energy is increased. The effect can be ascribed to the increase of the LA thermal budget. Interestingly, the amorphous HfO_2 layer was maintained in the present sample (with LA at 600 mJ/cm^2), resulting from the decrease of heat absorption. GIXRD results also reveal that the laser-annealed HfO_2 layer retains its amorphous structure as the crystallization peak ($2\Theta = \sim 29°$) of HfO_2 is not observed in Fig. 2i.[12] An Al capping layer on the Ti electrode, with its high reflectivity, is suggested for the above maintenance.

Kim et al.[4] demonstrated the effect of oxygen gettering on a Ti electrode. The oxygen diffusivity of the metal oxide layer is very fast, about $\sim 10^{-16}$ cm^2/s at a temperature of 300 K. In addition, the Ti electrode easily absorbed the oxygen after FGA due to the low electronegativity value of 1.54. Thus, the Ti electrode absorbed oxygen from the IL through the HfO_2 layer after FGA. Finally, a small amount of oxygen vacancies formed in the HfO_2 layer, and the remaining Si layer in IL then grew in the form of an epitaxial Si layer ($\sim$4 Å). Compared with the control sample in Fig. 2e, this layer can be clearly observed in the present samples with and without LA, as shown in Fig. 2f-h. A Ti nMOS capacitor experienced no significant increase in D_{it} after oxygen gettering in IL.[5] The regrowth of the epitaxial Si layer is attributed to the decrease in the EOT of $\sim$11.7 Å without a significant increase in D_{it} (sample with the LA at 600 mJ/cm^2).

Figure 3 shows (a) drain current vs drain voltage (I_{DS}–V_{DS}) and (b) drain current vs gate voltage (I_{DS}–V_{GS}) graphs of the laser-annealed HfO_2/SiO_2 nMOSFET with Ti electrode. Well-defined linear and saturation regions were observed in the I_{DS}–V_{DS} graph. This means that LA is sufficient for the source/drain activation process where degradation of the Ti electrode is almost negligible. Moreover, a good subthreshold swing (S.S.) value ($\sim$70 mV/dec) was also demonstrated in the I_{DS}–V_{GS} graph. The S.S. value is similar to that in SiO_2 nMOSFETs. Based on the above results, it can be

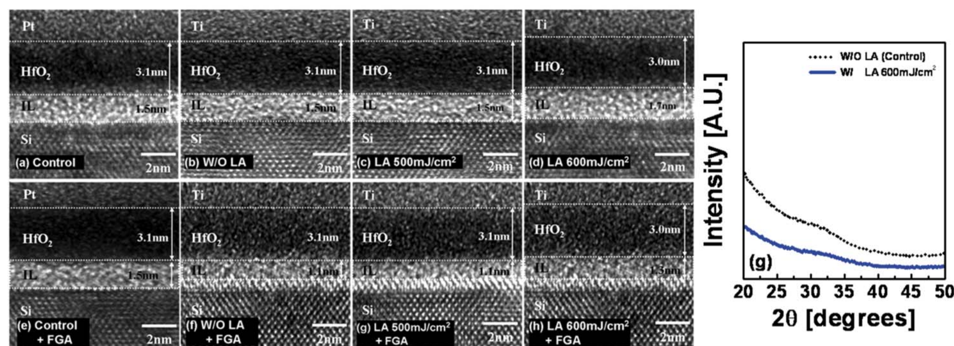

Figure 2. (Color online) HR-XTEM analyses of the samples: (a) control (Pt electrode), (b) Ti W/O LA, (c) Ti W/ LA 500 mJ/cm^2, (d) Ti W/ LA 600 mJ/cm^2, (e) control + FGA, (f) Ti W/O LA + FGA, (g) Ti W/LA 500 mJ/cm^2 + FGA, and (h) Ti W/LA 600 mJ/cm^2 + FGA. GIXRD results (i) of samples W or W/O LA at 600 mJ/cm^2.

Downloaded 11 Aug 2008 to 61.72.111.1. Redistribution subject to ECS license or copyright; see http://www.ecsdl.org/terms_use.jsp

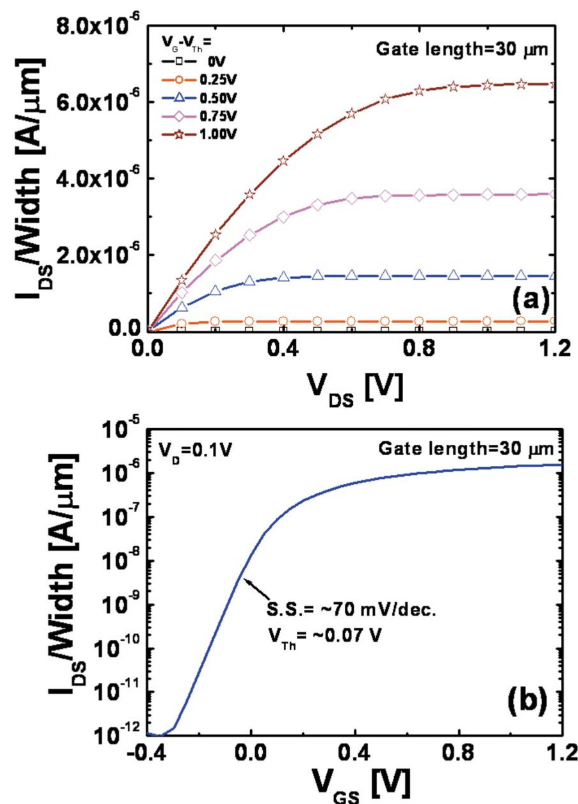

Figure 3. (Color online) (a) I_{DS}–V_{DS} and (b) I_{DS}–V_{GS} characteristics of laser-annealed (at 600 mJ/cm^2) HfO_2/SiO_2 nMOSFET with Ti electrode. The gate length/width is 30/20 μm. The threshold voltage (V_{th}) and S.S. are ~0.07 V and ~70 mV/dec, respectively.

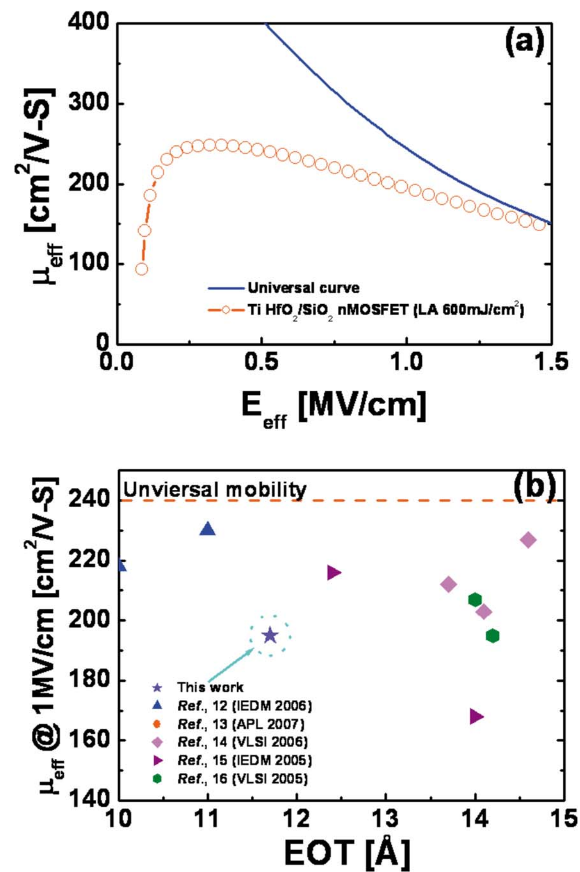

Figure 4. (Color online) (a) Electron mobility vs electric field plot for laser-annealed HfO_2/SiO_2 nMOSFET with Ti electrode. (b) Electron mobility at 1 MV/cm^2 vs EOT (Å). The closed and open symbols denote this experiment and reported results, respectively. The reported results were obtained by metal gate/HfO_2 nMOSFET.

deduced that LA does not induce serious degradation of the HfO_2/SiO_2 nMOSFET with Ti electrode.

Figure 4a shows the effective mobility curve of the laser-annealed HfO_2/SiO_2 nMOSFET samples (600 mJ/cm^2, Ti electrode). The peak value of the effective mobility is ~250 cm^2/V s. Thus, the laser-annealed HfO_2/SiO_2 nMOSFET with Ti electrode can achieve a mobility of ~195 cm^2/V s which is almost equal to 80% of the universal mobility for SiO_2. Figure 4b shows the effective mobility at 1 MV/cm^2 vs EOT (Å) obtained from the present experiment as well as from the reported results.[12-16] Compared with reported results, the present laser-annealed sample shows slightly lower effective mobility. The mobility is related to the surface roughness, interface quality, and the fixed charge in the oxide. Based on our HR-XTEM image, the laser-annealed sample shows a flat surface after FGA. Ti electrode does not significantly affect the interface trap density. This decrease in the effective mobility can be attributed to the additional fixed charge in the HfO_2 layer that is caused by the existence of oxygen vacancies after FGA. This low effective mobility will be improved to control the concentration of oxygen in the HfO_2 layer through additional oxygen annealing.

Conclusions

In summary, the effect of LA on HfO_2/SiO_2 nMOSFETs with Ti electrode is demonstrated. LA can effectively reduce the degradation of Ti electrode and retard crystallization of the HfO_2 layer. The effect of oxygen gettering in IL after FGA can be confirmed by HR-XTEM analysis. The LA sample has an effective work function (~4.26 eV) of the conduction bandedge and its mobility is equal to 80% of the universal mobility for SiO_2. Therefore, LA can be considered as a promising method for applications to metal gate electrodes with high-*k* dielectric.

Acknowledgments

This work was supported by the Center for Distributed Sensor Network at Gwangju Institute of Science and Technology.

Gwangju Institute of Science and Technology assisted in meeting the publication costs of this article.

References

1. C. C. Hobbs, L. R. C. Fonseca, A. Knizhnik, V. Dhandapani, S. B. Samavedam, W. J. Tayer, J. M. Grant, L. G. Dip, D. H. Triyoso, R. I. Hegde, et al., *IEEE Trans. Electron Devices*, **51**, 971 (2004).
2. Q. Lu, Y. C. Yeo, P. Ranade, H. Takeuchi, T. J. King, and C. Hu, *Symposium VLSI Technical Digest*, **2000**, 72.
3. H. B. Michaelson, *J. Appl. Phys.*, **48**, 4729 (1997).
4. H. Kim, P. C. McIntyre, C. O. Chui, K. C. Sarawat, and S. Stemmer, *J. Appl. Phys.*, **96**, 3467 (2004).
5. K. I. Seo, D. I. Lee, P. Pianetta, H. Kim, K. C. Sarawat, and P. C. McIntyre, *Appl. Phys. Lett.*, **89**, 142912 (2006).
6. K. H. Weiner, P. G. Carey, A. M. McCarthy, and T. W. Sigmon, *IEEE Electron Device Lett.*, **13**, 369 (1992).
7. Q. Zhang, J. Huang, N. Wu, G. Chen, M. Hong, L. K. Bera, and C. Zhu, *IEEE Electron Device Lett.*, **27**, 728 (2006).
8. S. Heo, H. Hwang, H. T. Cho, and W. A. Krull, *Appl. Phys. Lett.*, **89**, 243516 (2006).
9. J. R. Hauser and K. Ahmed, *Characterization and Metrology for ULSI Technology: 1998 International Conference*, D. G. Seiler, A. C. Diebold, W. M. Bullis, T. J. Shaffner, R. McDonald, and E. J. Walters, Editors, pp. 235–239, AIP, New York (1998).
10. G. Bersuker, J. Barnett, N. Moumen, B. Foran, C. D. Yong, P. Lysaght, J. Peterson, B. H. Lee, P. M. Zeitzoff, and H. R. Huff, *Jpn. J. Appl. Phys., Part 1*, **43**, 7899 (2004).
11. D. C. Gilmer, J. K. Schaeffer, W. J. Taylor, G. Spencer, D. H. Triyoso, M. Raymond, D. Roan, J. Smith, C. Capsso, R. I. Hegde, et al., in *Proceedings of ESSDERC 2006*, p. 351 (2006).

Downloaded 11 Aug 2008 to 61.72.111.1. Redistribution subject to ECS license or copyright; see http://www.ecsdl.org/terms_use.jsp

12. P. D. Kirsch, M. A. Quevedo-Lopez, S. A. Krishnan, C. Krug, H. AlShareef, C. S. Park, R. Harris, N. Moumen, A. Neugroschel, G. Bersuker, et al., *Tech. Dig. - Int. Electron Devices Meet.*, **2006**, 1.
13. S. Guha, V. K. Paruchuri, M. Copel, V. Narayanan, Y. Y. Wang, P. E. Batson, N. A. Bojarczuk, B. Linder, and B. Doris, *Appl. Phys. Lett.*, **90**, 092902 (2007).
14. V. Narayanan, V. K. Paruchuri, N. A. Bojarczuk, B. P. Linder, B. Doris, Y. H. Kim, S. Zafar, J. Stathis, S. Brown, J. Arnold, et al., *Symposium VLSI Technical Digest*, **2006**, 178.
15. Y. T. Hou, F. Y. Yen, P. F. Hsu, V. S. Chang, P. S. Lim, C. L. Hung, L. G. Yao, J. C. Jiang, H. J. Lin, Y. Jin, et al., *Tech. Dig. - Int. Electron Devices Meet.*, **2005**, 31.
16. B. Doris, Y. H. Kim, B. P. Linder, M. Steen, V. Narayanan, D. Boyd, J. Rubino, L. Chang, J. Sleight, A. Topol, et al., *Symposium VLSI Technical Digest*, **2005**, 214.

Downloaded 11 Aug 2008 to 61.72.111.1. Redistribution subject to ECS license or copyright; see http://www.ecsdl.org/terms_use.jsp